

## THEORETICAL INVESTIGATION ON FLEXURAL PERFORMANCE OF RC BEAMS STRENGTHENED EXTERNALLY BY CFRP

**Khairy Hassan Abdelkareem<sup>\*</sup>, Fayez Kaiser Abdelseed<sup>\*</sup>, and Mohamed Omar Sayed<sup>\*\*</sup>**

<sup>\*</sup> Professors, Civil Eng. Dept., Assiut University

<sup>\*\*</sup> Assistant Researcher, Construction Research Institute, National Water Research Center, Egypt

(Received October 23, 2011 Accepted November 22, 2011)

*In this paper an analytical model is presented for reinforced concrete beams externally reinforced with carbon fiber reinforced polymer (CFRP) laminates using finite element method adopted by ANSYS. The finite element models are developed using a smeared cracking approach for concrete and three dimensional layered elements for the CFRP composites. In particular, attaching unidirectional CFRP to the tension face of RC beams has provided an increase in the stiffness and load capacity of the structure. However, due to the brittle nature of unidirectional CFRP, the ductility of the beam decreases. Consequently, the safety of the structure is compromised, due to the reduction in ductility. The purpose of this research is to investigate the behavior of normal and high strength reinforced concrete beams strengthened with CFRP sheets. The major test parameters included the grade of concrete, the different dimensions of the beam and the tensile reinforcement ratio. Furthermore, change in the strength, ductility and toughness of the beams, as the grade of concrete, the dimensions of the beam and tensile reinforcement bar ratios are altered, are investigated. Fifty-four reinforced concrete beams were modeled and analyzed up to failure.*

**KEYWORDS:** Finite Element Model, CFRP, High Strength Concrete, Ductility, Strength, Toughness.

### INTRODUCTION

There are many existing structures, which do not fulfill specified requirements. This for example may be due to upgrading of the design standards, increased loading, corrosion of the reinforcement bars, construction errors or accidents such as earthquakes. To remedy for insufficient capacity the structures need to be replaced or retrofitted. Different types of strengthening materials are available in the market. Examples of these are Ferro cement, steel plates and fiber reinforced polymer (FRP) laminate. Retrofitting of reinforced concrete (RC) structures by bonding external steel and FRP plates or sheets is an effective method for improving structural performance under both service and ultimate load conditions. It is both environmentally and economically preferable to repair or strengthen structures rather than to replace them totally. With the development of structurally effective adhesives, there have been marked increases in strengthening using steel plates and FRP laminates. FRP has

become increasingly attractive compared to steel plates due to its advantageous low weight, high stiffness and strength to weight ratio, corrosion resistance, lower maintenance costs and faster installation time. Earlier research has demonstrated that the addition of carbon fiber reinforced polymer (CFRP) laminate to reinforced concrete beams can increase stiffness and maximum load of the beams. There are several theoretical and experimental studies concerning the structural behavior of RC elements strengthened with CFRP, for examples reference [1,2,3,4,5]. In a study by N. F. Grace [6] the ultimate load carrying capacity of beams can be doubled by using a proper combination of horizontal and vertical fibers coupled with the proper epoxy and extending the vertical layers over the entire span of the beam reduces the diagonal cracks so that the longitudinal fibers are fully used and the load carrying capacity of the beams is significantly increased. Another study by Amer M. Ibrahim [7] the results obtained demonstrate that carbon fiber polymer is efficient more than glass fiber polymer in strengthening the reinforced concrete beams for shear. Other studies have also been conducted by J. Lundqvist [8] showed that the critical anchorage length for the sheet cannot clearly be established, however, there is a tendency that the critical anchorage length is less than 200 mm. At an anchorage length of 200 mm for the plate, the results showed that a critical anchorage length is attained. Increasing the anchorage length adds safety to the structure but does not increase the load carrying capacity. Yasmeen Taleb Obaidat [9] showed that the stiffness of the CFRP retrofitted beams is increased compared to that of the control beams. Employing externally bonded CFRP plates resulted in an increase in maximum load and the crack width for the retrofitted beams is decreased compared to the control beams. Also Mohammed Jassam [10] showed that analytical study explained that the best location of CFRP plate in strengthened beam is at edges and the location of CFRP plate is more effective than the number of CFRP plate layers on the flexural behavior of RC beam. Reza Mahjoub [11] indicated that the significant increase in the flexural strength can be achieved by bonding CFRP sheets to the tension face of high strength reinforced concrete beams. The gain in the ultimate flexural strength was more significant in beams with lower steel reinforcement ratios, also he found that for all strengthened test beams, the tensile steel strains were always higher than the CFRP strains and the effect of the strengthening plate is to reduce strain in the compression fibers of the concrete. Compared to a beam reinforced heavily with steel only, beams reinforced with both steel and CFRP have adequate deformation capacity, in spite of their brittle mode of failure. As the amount of tensile steel reinforcement increases, the additional strength provided by the carbon FRP external reinforcement decreases.

## **NUMERICAL APPROACH**

A large number of available software like DIANA, ABAQUS, and ANSYS etc. incorporate finite elements based analysis. In this paper an attempt has been made with ANSYS (version 11) [12] software to bring into focus the versatility and powerful analytical capabilities of finite elements technique by objectively modeling the complete response of analysis beams. The finite elements model uses a smeared cracking approach to model the reinforced concrete and three dimensional layered elements to model the fiber reinforced polymer FRP composites. This model can help to confirm the theoretical calculations as well as to provide a valuable supplement to the laboratory investigation of behavior.

## FINITE ELEMENT MODELS

The FEM calibration study included modeling a concrete beam with the dimensions and properties. Due to the symmetry of cross-section of the concrete beam and loading, symmetry was utilized in the FEM; only one quarter of the beam was modeled. To create the finite element model in ANSYS there are multiple tasks that have to be completed for the model to run properly. Models can be created using command prompt line input or the Graphical User Interface (GUI). For this model, the GUI was utilized to create the model.

## ELEMENTTYPES

### Reinforced Concrete:

An eight-node solid element, Solid65, was used to model the concrete. The solid element has eight nodes with three degrees of freedom at each node – translations in the nodal  $x$ ,  $y$ , and  $z$  directions. The element is capable of plastic deformation, cracking in three orthogonal directions, and crushing. The geometry and node locations for this element type are shown in Figure 1.

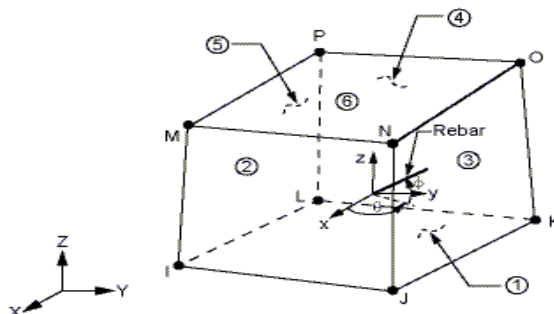


Figure 1: Solid65 – 3-D reinforced concrete solid (ANSYS)

### Reinforcing steel:

Modeling of reinforcing steel in finite elements is much simpler than the modeling of concrete. A Link8 element was used to model steel reinforcement. This element is a 3D spar element and it has two nodes with three degrees of freedom – translations in the nodal  $x$ ,  $y$ , and  $z$  directions. This element is also capable of plastic deformation. A perfect bond between the concrete and steel reinforcement is considered. However, in the present study the steel reinforcing was connected between nodes of each adjacent concrete solid element, so the two materials shared the same nodes.

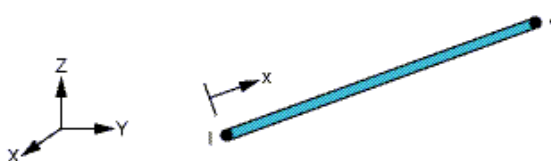


Figure 2: Link8 – 3-D spar (ANSYS)

### Steel plate:

Steel plates were added at support and loading locations in the finite element models (as in the actual beams) in order to avoid stress concentration problems. An elastic modulus equal to  $2000,000 \text{ kg/cm}^2$  and Poisson's ratio of  $0.3$  were used for the plates. The steel plates were assumed to be linear elastic materials. A Solid 45 element was used to model steel plates. The geometry and node locations for this element type are shown in figure 3.

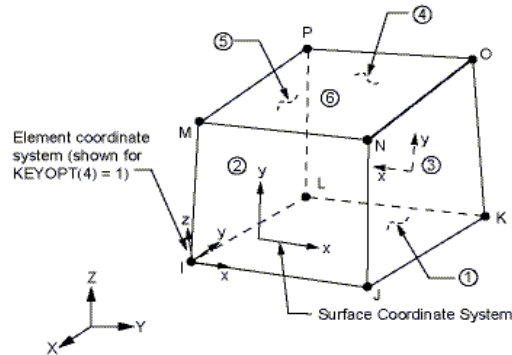


Figure 3: Solid45 – 3-D solid (ANSYS)

### CFRP Laminates:

A layered solid element, Solid46, was used to model the FRP composites. The element allows for up to 250 different material layers with different orientations and orthotropic material properties in each layer. The element has three degrees of freedom at each node and translations in the nodal x, y, and z directions. The geometry, node locations, and the coordinate system are shown in Figure 4. As the epoxy is usually stronger than the concrete, perfect bond between FRP and concrete was assumed.

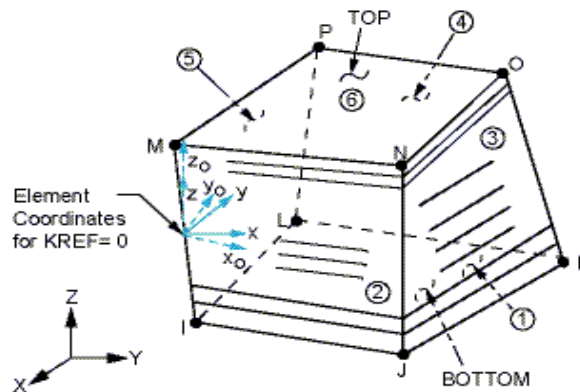


Figure 4: Solid46 – 3-D layered structural solid (ANSYS)

### MATERIAL PROPERTIES:

#### Concrete:

For the full-scale beam tests (Kachlakev and McCurry 2000) [13], an effort was made to accurately estimate the actual elastic modulus of the beams using the ultrasonic pulse velocity method (ASTM 1983, ASTM 1994). A correlation was made between pulse velocity and compressive elastic modulus following the ASTM standard methods. From this work, it was noted that each experimental beam had a slightly different elastic modulus; therefore, these values were used in the finite element modeling. From the elastic modulus obtained by the pulse velocity method, the ultimate concrete compressive and tensile strengths for each beam model were calculated by Equations 1 and 2 respectively (ACI 318, 1999).

$$f'c = \left( \frac{Ec}{57000} \right)^2 \dots\dots (1)$$

$$fr = 7.5 \sqrt{f'c} \dots\dots (2)$$

where:

Ec : Elastic modulus.

f'c : Ultimate uniaxial compressive strength

fr : Ultimate uniaxial tensile strength (modulus of rupture).

Where Ec, f'c and fr are in psi.

Poisson's ratio for concrete was assumed to be 0.2 for all beams. Shear transfer coefficient (βt) represents conditions of the crack face. The value of βt ranges from 0.0 to 1.0, with 0.0 representing a smooth crack (complete loss of shear transfer) and 1.0 representing a rough crack (no loss of shear transfer). The shear transfer coefficient used in present study varied between 0.3 and 0.8. The ANSYS program requires the uniaxial stress-strain relationship for concrete in compression. Equations 3 and 4 were used along with Equation 5 to construct the uniaxial compressive stress-strain curve for concrete in this study.

$$f = \frac{Ec \epsilon}{1 + \frac{\epsilon}{\epsilon_0}} \dots\dots (3)$$

$$\epsilon_0 = \frac{2f'c}{Ec} \dots\dots (4)$$

$$Ec = \frac{f}{\epsilon} \dots\dots (5)$$

where:

f = stress at any strain ε , psi

ε = strain at stress f

ε<sub>0</sub> = strain at the ultimate compressive strength f'c

Figure 5 shows the simplified compressive uniaxial stress-strain relationship that was used in this study.

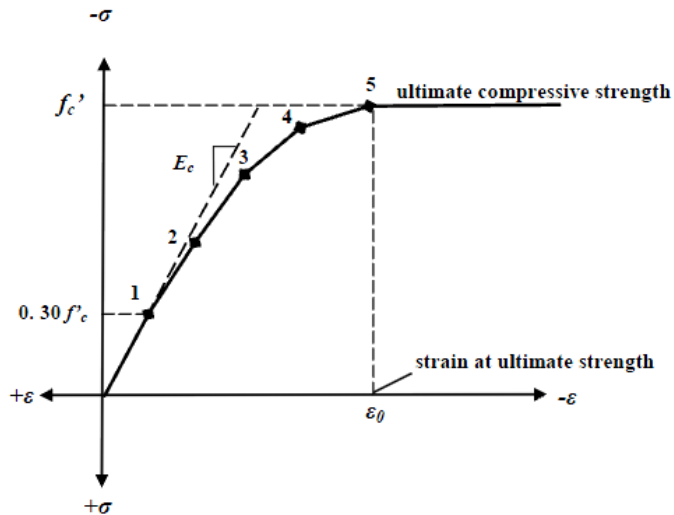


Figure 5: Simplified compressive uniaxial stress-strain curve for concrete.

### Failure Criteria for Concrete:

The model is capable of predicting failure for concrete materials. Both cracking and crushing failure modes are accounted for. The two input strength parameters – i.e., ultimate uniaxial tensile and compressive strengths – are needed to define a failure surface for the concrete.

A three-dimensional failure surface for concrete is shown in Figure 6. The most significant nonzero principal stresses are in the  $x$  and  $y$  directions, represented by  $\sigma_{xp}$  and  $\sigma_{yp}$ , respectively. Three failure surfaces are shown as projections on the  $\sigma_{xp}$ - $\sigma_{yp}$  plane. The mode of failure is a function of the sign of  $\sigma_{zp}$  (principal stress in the  $z$  direction). For example, if  $\sigma_{xp}$  and  $\sigma_{yp}$  are both negative (compressive) and  $\sigma_{zp}$  is slightly positive (tensile), cracking would be predicted in a direction perpendicular to  $\sigma_{zp}$ . However, if  $\sigma_{zp}$  is zero or slightly negative, the material is assumed to crush (ANSYS).

In a concrete element, cracking occurs when the principal tensile stress in any direction lies outside the failure surface. After cracking, the elastic modulus of the concrete element is set to zero in the direction parallel to the principal tensile stress direction. Crushing occurs when all principal stresses are compressive and lie outside the failure surface; subsequently, the elastic modulus is set to zero in all directions (ANSYS), and the element effectively disappears. During this study, it was found that if the crushing capability of the concrete is turned on, the finite element beam models fail prematurely. Crushing of the concrete started to develop in elements located directly under the loads. Subsequently, adjacent concrete elements crushed within several load steps as well, significantly reducing the local stiffness. Finally, the model showed a large displacement, and the solution diverged.

A pure “compression” failure of concrete is unlikely. In a compression test, the specimen is subjected to a uniaxial compressive load. Secondary tensile strains induced by Poisson’s effect occur perpendicular to the load. Because concrete is relatively weak in tension, these actually cause cracking and the eventual failure. Therefore, in

this study, the crushing capability was turned off and cracking of the concrete controlled the failure of the finite element models.

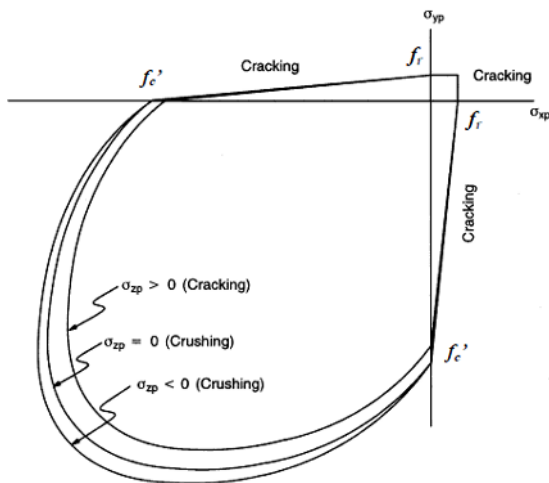


Figure 6: 3-D failure surface for concrete (ANSYS)

### Steel Reinforcement and Steel Plates:

The steel for the finite element models was assumed to be an elastic-perfectly plastic material and identical in tension and compression. Poisson’s ratio of 0.3 was used for the steel reinforcement in this study. Figure 7 shows the stress-strain relationship used in this study. Material properties for the steel reinforcement for all four models are as follows:

Elastic modulus,  $E_s = 2000,000 \text{ Kg/cm}^2$

Yield stress,  $f_y = 3600 \text{ Kg/cm}^2$

Poisson’s ratio,  $\nu = 0.3$

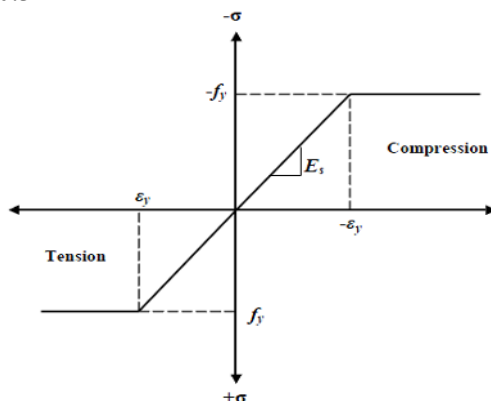


Figure 7: Stress-strain curve for steel reinforcement

### FRP Composites:

FRP composites are materials that consist of two constituents. The constituents are combined at a macroscopic level and are not soluble in each other. One constituent is

the reinforcement, which is embedded in the second constituent, a continuous polymer called the matrix (Kaw 1997) [14]. The reinforcing material is in the form of fibers, i.e., carbon and glass, which are typically stiffer and stronger than the matrix. The FRP composites are anisotropic materials; that is, their properties are not the same in all directions. Figure 8 shows a schematic of FRP composites.

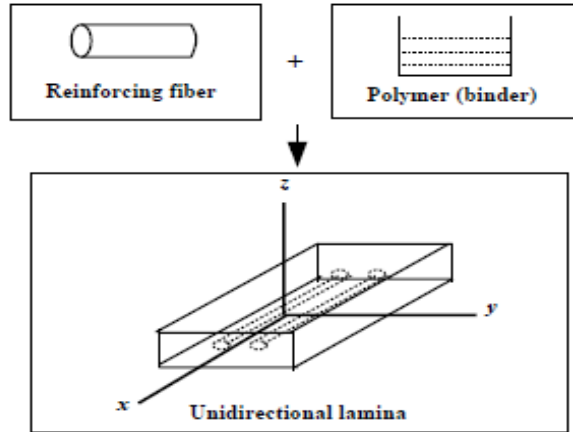


Figure 8: Schematic of FRP composites.

Input data needed for the CFRP composites in the finite element models are as follows:

- Number of layers.
- Thickness of each layer.
- Orientation of the fiber direction for each layer.
- Elastic modulus of the FRP composite in three directions ( $E_x$ ,  $E_y$  and  $E_z$ ).
- Shear modulus of the FRP composite for three planes ( $G_{xy}$ ,  $G_{yz}$  and  $G_{xz}$ ).
- Major Poisson's ratio for three planes ( $\nu_{xy}$ ,  $\nu_{yz}$  and  $\nu_{xz}$ ).

**Table1: summary of material properties for CFRP composite.**

FRP composite	Elastic modulus $\text{Kg/ cm}^2$	Major poison's ratio	Shear modulus $\text{Kg/ cm}^2$
Carbon fiber reinforced polymer	$E_x=620000$	$\nu_{xy}=0.22$	$G_{xy}=32700$
	$E_y=480000$	$\nu_{xz}=0.22$	$G_{xz}=32700$
	$E_z=480000$	$\nu_{yz}=0.30$	$G_{yz}=18600$

### Geometry of the beams:

Fifty four beams will be analyzed using the proposed ANSYS finite elements model.

Table 2,3 and 4 shows all beams evaluated in the present study. Twenty seven beams were strengthening by CFRP as shown in Figure 9.



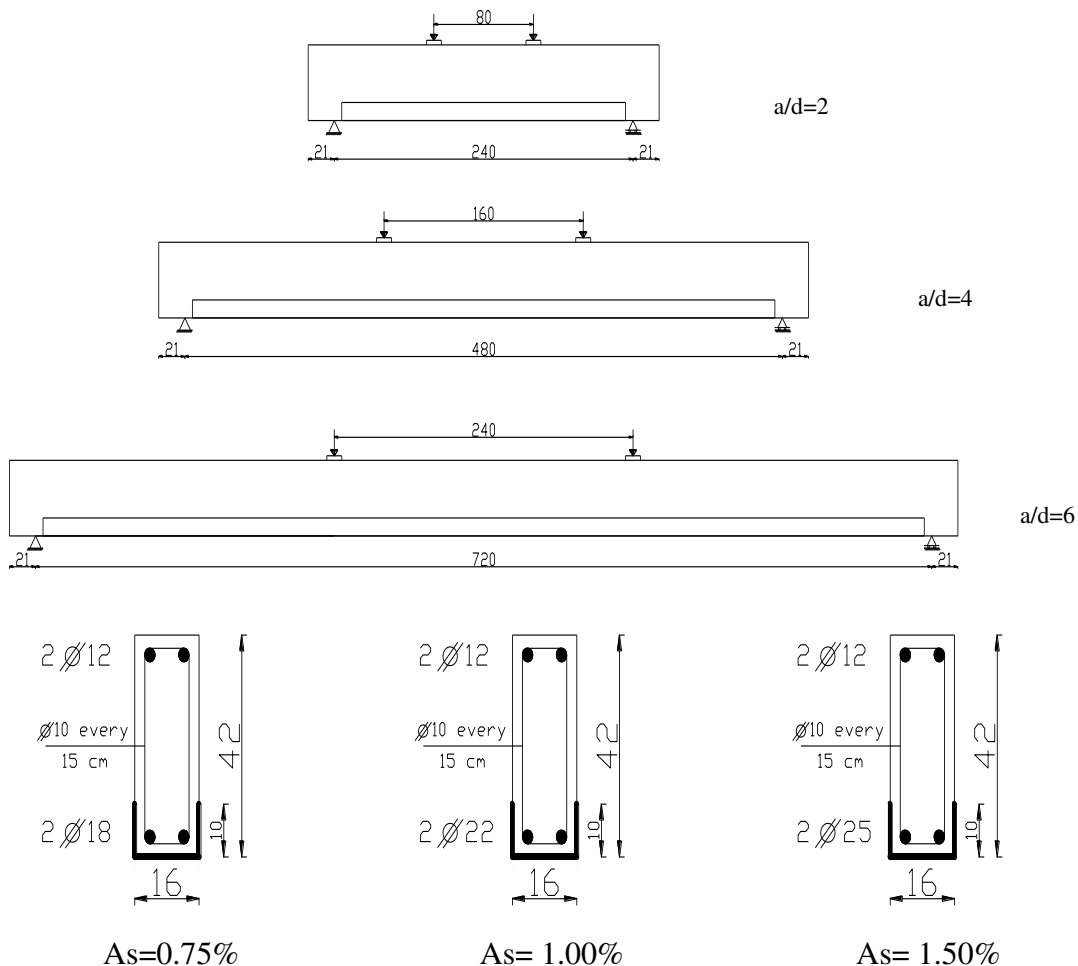


Figure 9: Dimensions and Reinforcement of beams.

\*All dimension in cm

All beams are strengthened by one layer of CFRP laminates which it have 1mm thickness as shown in figure 9.

Due to the symmetry in cross-section of the concrete beam and loading, symmetry was utilized in the finite elements analysis; only one quarter of the beam was modeled. This approach reduced computational time and computer disk space requirements significantly. The finite element mesh, boundary condition and loading regions of all beams are shown in Figure 10.

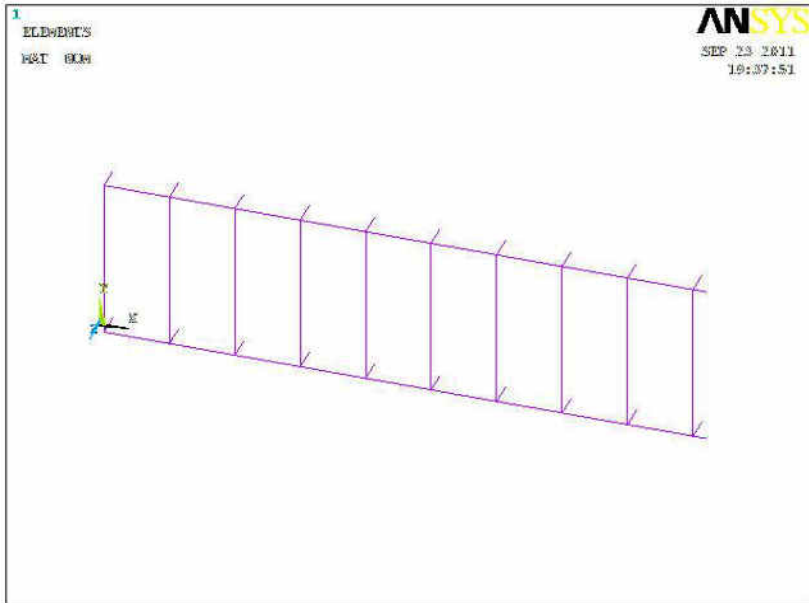
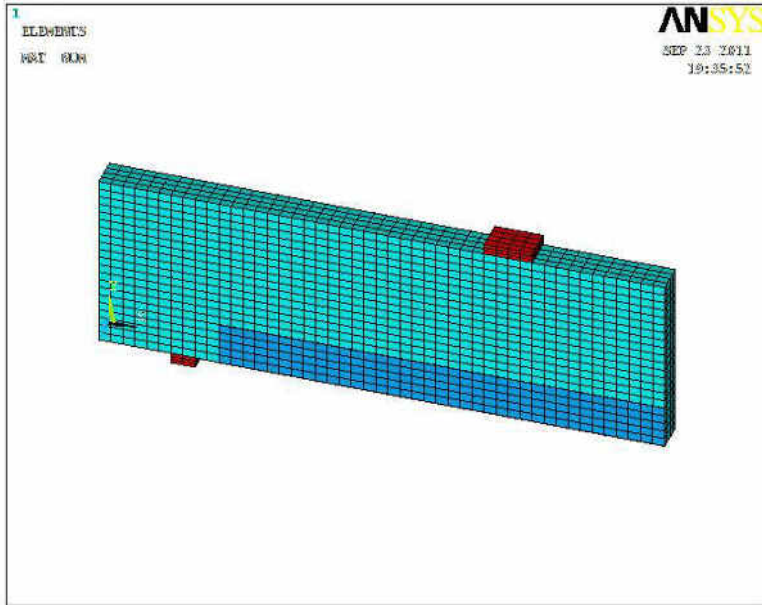


Figure 10: Finite element mesh, boundary condition and loading regions for a quarter beam model of all beams.

Table 2, Table 3 and Table 4 shows a summary of Analyzed beams and the parameters that effect on it.

**Table 2: Group (A)**

No.	Grade	a/d	As%	S	Analyzed Beams	
					Control Beam	Strengthening Beam
1	200	2	0.75%	15	A1a	A1b
2			1.00%		A2a	A2b
3			1.50%		A3a	A3b
4		4	0.75%		A4a	A4b
5			1.00%		A5a	A5b
6			1.50%		A6a	A6b
7		6	0.75%		A7a	A7b
8			1.00%		A8a	A8b
9			1.50%		A9a	A9b

**Table 3: Group (B)**

No.	Grade	a/d	As%	S	Analyzed Beams	
					Control Beam	Strengthening Beam
1	400	2	0.75%	15	B1a	B1b
2			1.00%		B2a	B2b
3			1.50%		B3a	B3b
4		4	0.75%		B4a	B4b
5			1.00%		B5a	B5b
6			1.50%		B6a	B6b
7		6	0.75%		B7a	B7b
8			1.00%		B8a	B8b
9			1.50%		B9a	B9b

**Table 4: Group (C)**

No.	Grade	a/d	As%	S	Analyzed Beams	
					Control Beam	Strengthening Beam
1	600	2	0.75%	15	C1a	C1b
2			1.00%		C2a	C2b
3			1.50%		C3a	C3b
4		4	0.75%		C4a	C4b
5			1.00%		C5a	C5b
6			1.50%		C6a	C6b
7		6	0.75%		C7a	C7b
8			1.00%		C8a	C8b
9			1.50%		C9a	C9b

Where:

Grade : grade of concrete.

- $a/d$  : the shear span to depth ratio.  
 $A_s$  : the percentage of the steel in concrete.  
 $S$  : spacing between stirrups.

### Result and analysis:

As examples of the obtained results, figures 11, 12 and 13 illustrated load deflection curves for beams (A2, A5, and A8) group A

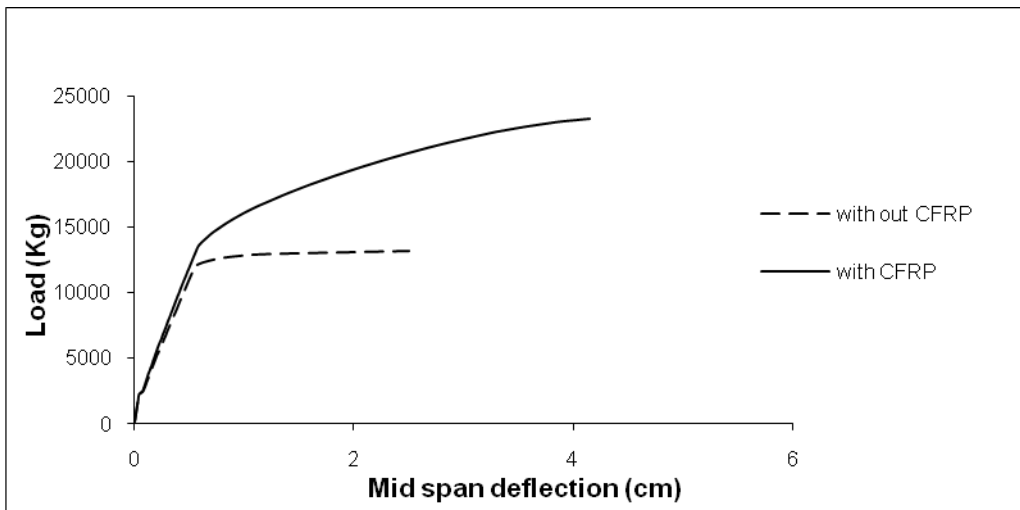


Figure 11: Load - Deflection curve for beam A2

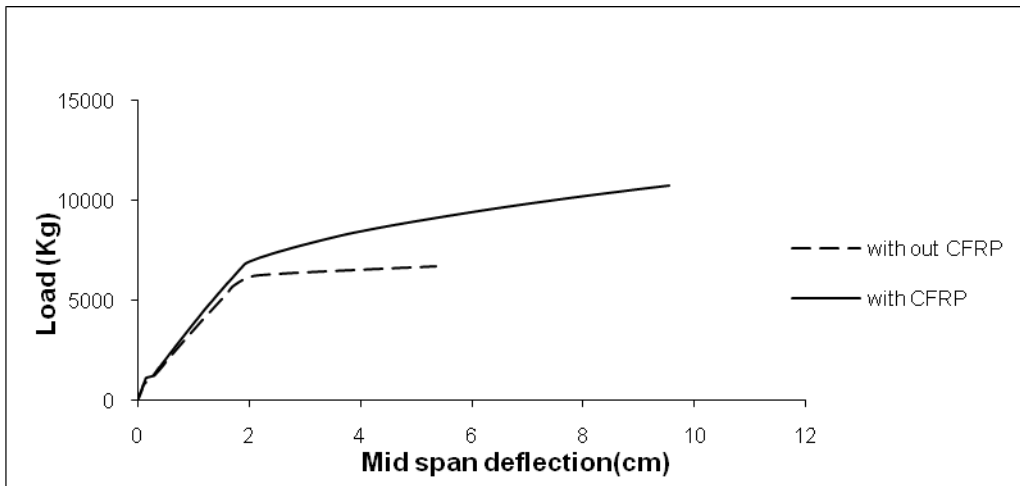


Figure 12: Load - Deflection curve for beam A5

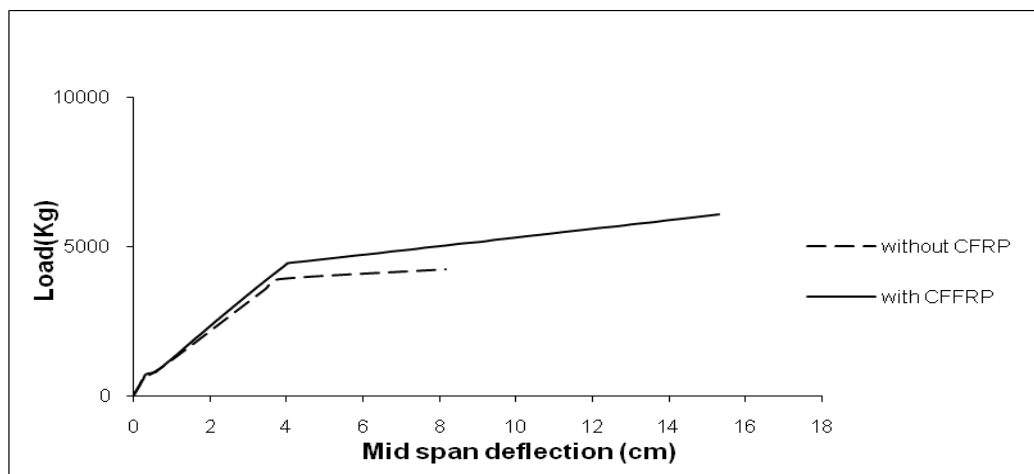


Figure 13: Load - Deflection curve for beam A8

Figures 14, 15 and 16 illustrated load deflection curves for beams (B2, B5, and B8) from group B

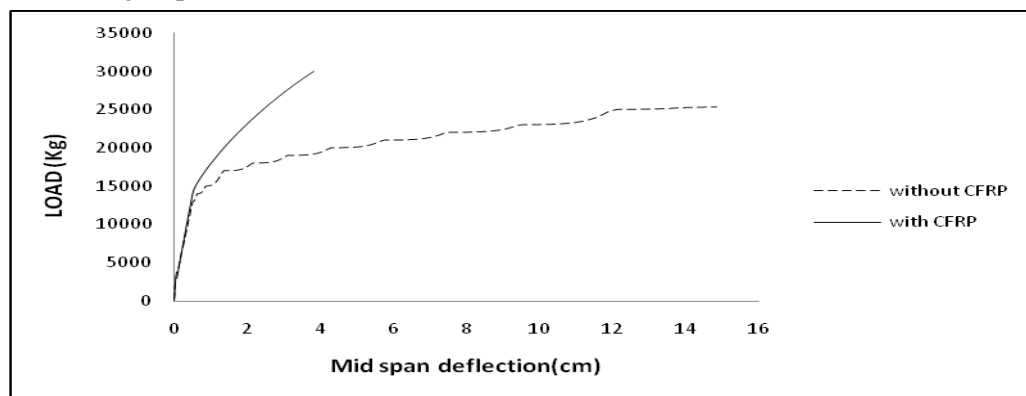


Figure 14: Load - Deflection curve for beam B2

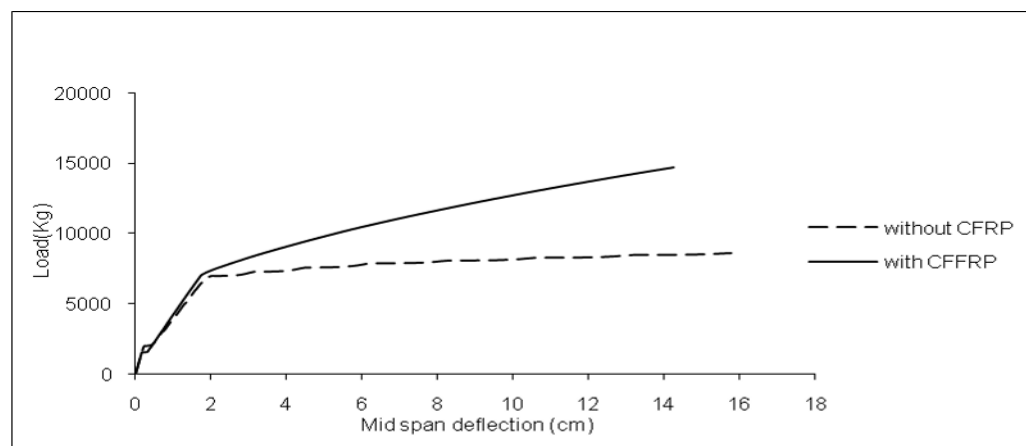


Figure 15: Load - Deflection curve for beam B5

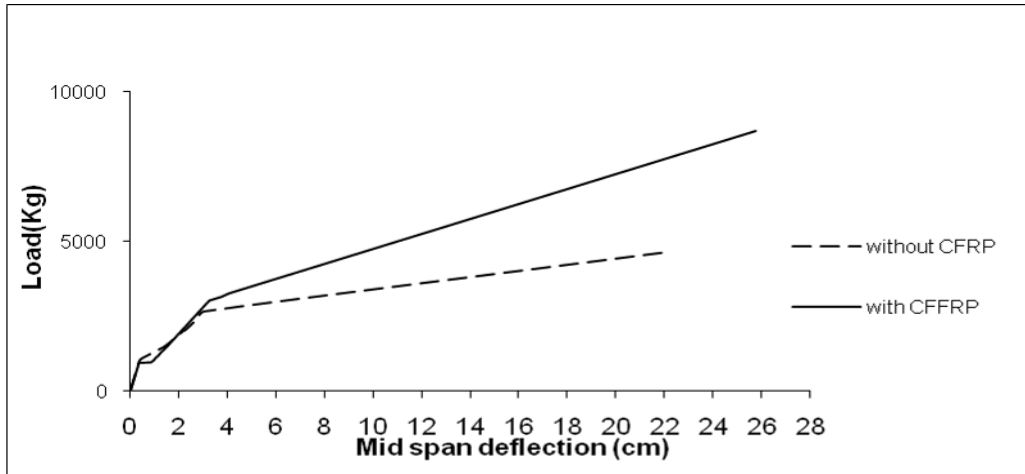


Figure 16: Load - Deflection curve for beam B8

Figures 17, 18 and 19 illustrated load deflection curves for beams (C2, C5, and C8) from group C

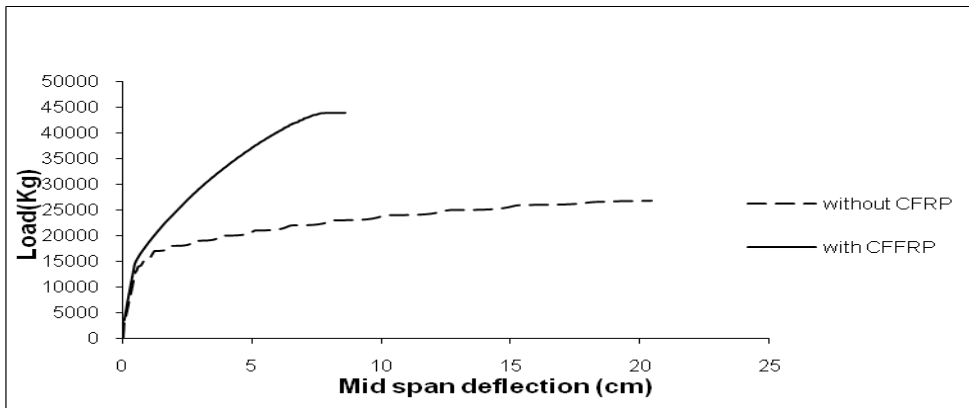


Figure 17: Load - Deflection curve for beam C2

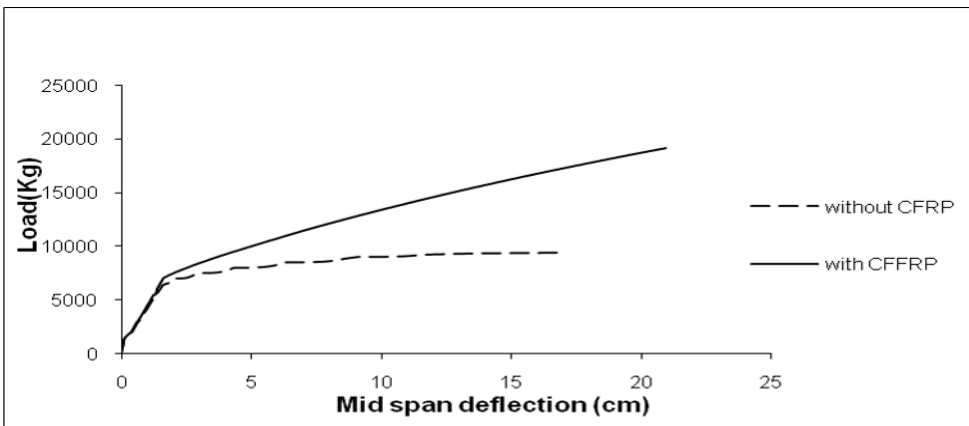


Figure 18: Load - Deflection curve for beam C5

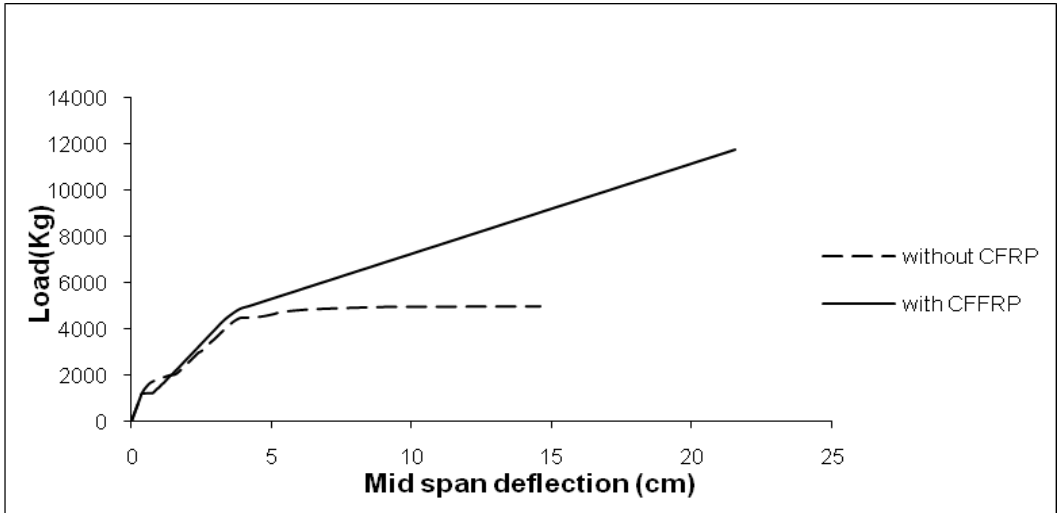


Figure 19: Load - Deflection curve for beam C8

From these results we carried out numerical analysis in figure20:

**For grade 200 of concrete:**

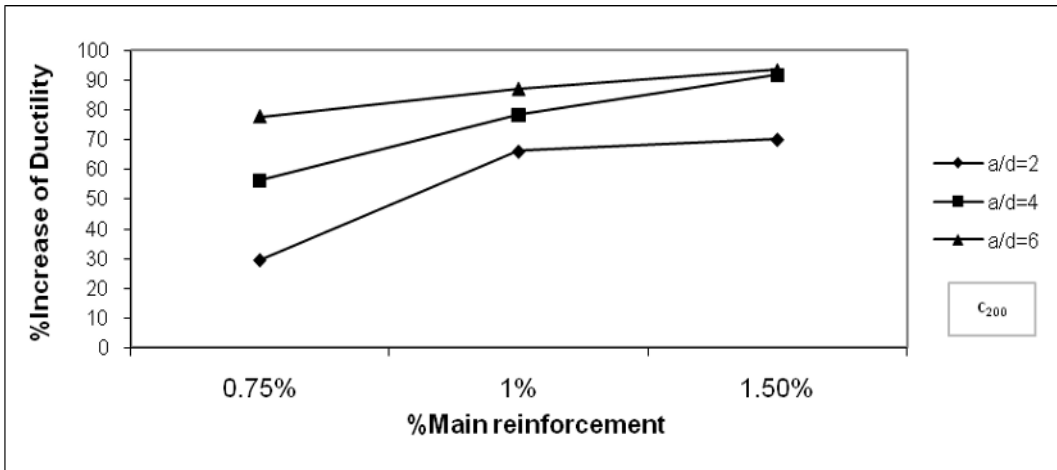


Figure 20: relation between %increase of ductility and %main reinforcement.

The relation of figure 20 can be represented by the following equations:

$$D1 = 0.20A_s + 0.15R = 0.91 \quad a/d=2 \quad \dots\dots (6)$$

$$D2 = 0.18A_s + 0.40 \quad R = 0.99 \quad a/d=4 \quad \dots\dots (7)$$

$$D3 = 0.08A_s + 0.70 \quad R = 0.99 \quad a/d=6 \quad \dots\dots (8)$$

Equations 6, 7 and 8 are represented by:

$$\%D = a_0 + a_1 A_s \quad \dots\dots (9)$$

$a_0, a_1$  depend on  $a/d$  ratio as :

$$a_0 = 0.14(a/d) - 0.13 \quad R = 0.99 \quad \dots\dots (10)$$

$$a_1 = 0.27 - 0.03(a/d) \quad R = 0.93 \quad \dots\dots (11)$$

By substitution in equation (9)

$$\%D = 0.14(a/d) - 0.13 + [0.27 - 0.03(a/d)] A_s \quad \dots\dots (12)$$

Following the same procedures:

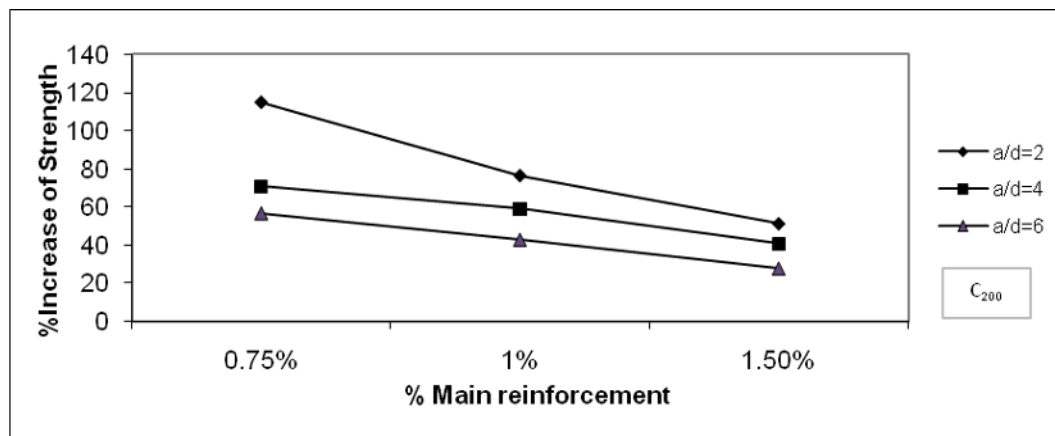


Figure 21: relation between % increase of strength and % main reinforcement.

The relation of figure 21 can be represented by the following equations:

$$S1 = -0.33A_s + 1.44 \quad R=0.99 \quad a/d=2 \quad \dots\dots (13)$$

$$S2 = -0.15A_s + 0.87 \quad R=0.99 \quad a/d=4 \quad \dots\dots (14)$$

$$S3 = -0.14A_s + 0.71 \quad R=0.99 \quad a/d=6 \quad \dots\dots (15)$$

Equations 13, 14 and 15 are represented by:

$$\% S = a_0 + a_1 A_s \quad \dots\dots (16)$$

$a_0, a_1$  depend on  $a/d$  ratio as:

$$a_0 = 1.74 - 0.18(a/d) \quad R=0.95 \quad \dots\dots (17)$$

$$a_1 = -0.65 + 0.21(a/d) - 0.02(a/d)^2 \quad R=1.00 \quad \dots\dots (18)$$

By substitution in equation (16)

$$\%S = 1.74 - 0.18(a/d) + [-0.02(a/d)^2 + 0.21(a/d) - 0.65] A_s \quad \dots\dots (19)$$

Following the same procedures:

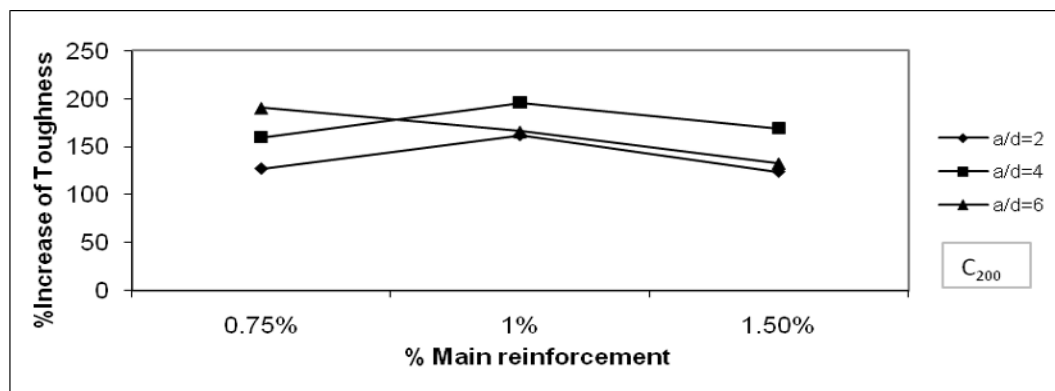


Figure 22: relation between % increase of toughness and % main reinforcement.

The relation of figure 22 can be represented by the following equations:



$$T1 = -0.37A_s^2 + 1.46A_s + 0.18 \quad R=1 \quad a/d=2 \quad \dots\dots (20)$$

$$T2 = -0.31A_s^2 + 1.29 A_s + 0.62 \quad R=1 \quad a/d=4 \quad \dots\dots (21)$$

$$T3 = -0.29A_s + 2.21 \quad R=0.99 \quad a/d=6 \quad \dots\dots (22)$$

Equation 20, 21 and 22 are represented by:

$$\% T = a_0 + a_1 A_s + a_2 A_s^2 \quad \dots\dots (23)$$

$a_0, a_1$  and  $a_2$  depend on  $a/d$  ratio as:

$$a_0 = 0.51(a/d) - 1.03 \quad R=0.95 \quad \dots\dots (24)$$

$$a_1 = -0.44(a/d) + 2.57 \quad R=0.91 \quad \dots\dots (25)$$

$$a_2 = 0.09(a/d) - 0.60 \quad R=0.93 \quad \dots\dots (26)$$

By substitution in equation (23)

$$\% T = 0.51(a/d) - 1.03 + [-0.44(a/d) + 2.57] A_s + [0.09(a/d) - 0.6] A_s^2 \quad \dots\dots (27)$$

**For grade 400 of concrete:**

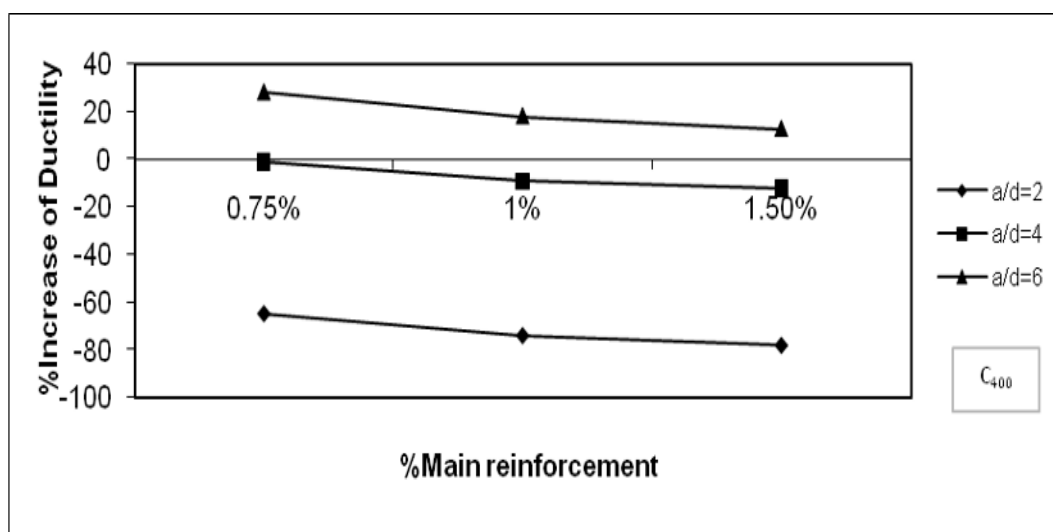


Figure 23: relation between % increase of ductility and % main reinforcement.

The relation of figure 23 can be represented by the following equations:

$$D4 = -0.07A_s - 0.60 \quad R=0.97 \quad a/d=2 \quad \dots\dots (28)$$

$$D5 = -0.06A_s + 0.03 \quad R=0.96 \quad a/d=4 \quad \dots\dots (29)$$

$$D6 = -0.08A_s + 0.35 \quad R=0.97 \quad a/d=6 \quad \dots\dots (30)$$

Equations 28, 29 and 30 are represented by:

$$\% D = a_0 + a_1 A_s \quad \dots\dots (31)$$

$a_0, a_1$  depend on  $a/d$  ratio as:

$$a_0 = 0.24(a/d) - 1.02 \quad R=0.98 \quad \dots\dots (32)$$

$$a_1 = -0.004(a/d)^2 + 0.03(a/d) - 0.11 \quad R=1 \quad \dots\dots (33)$$

By substitution in equation (31)

$$\% D = 0.24(a/d) - 1.01 + [-0.004(a/d)^2 + 0.03(a/d) - 0.11] A_s \quad \dots\dots (34)$$

Following the same procedures:

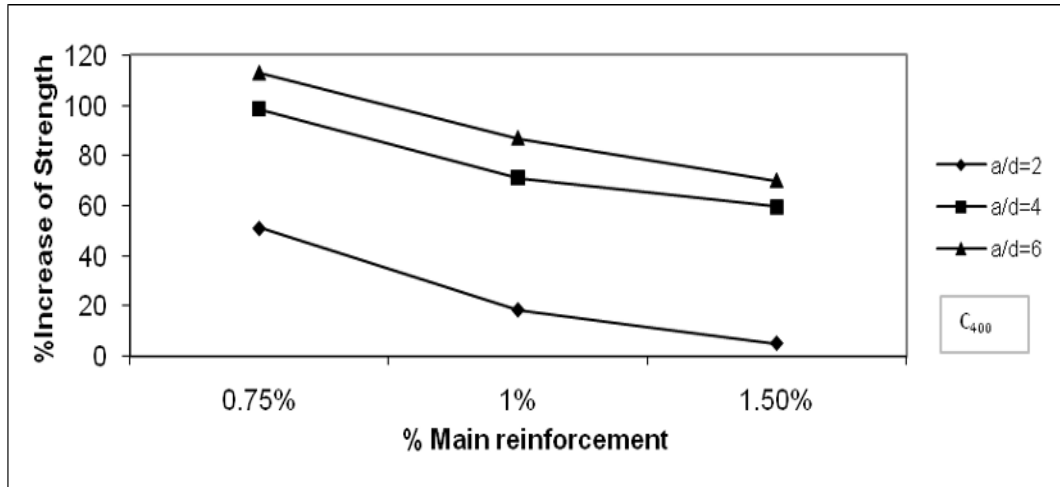


Figure 24: relation between % increase of strength and % main reinforcement.

The relation of figure 24 can be represented by the following equations:

$$S4 = -0.23A_s + 0.71 \quad R=0.97 \quad a/d=2 \quad \dots\dots (35)$$

$$S5 = -0.19A_s + 1.15 \quad R=0.97 \quad a/d=4 \quad \dots\dots (36)$$

$$S6 = -0.22A_s + 1.33 \quad R=0.99 \quad a/d=6 \quad \dots\dots (37)$$

Equations 35,36 and 37 are represented by:

$$\% S = a_0 + a_1 A_s \quad \dots\dots (38)$$

$a_0, a_1$  depend on  $a/d$  ratio as:

$$a_0 = 0.16 (a/d) + 0.44 \quad R=0.97 \quad \dots\dots (39)$$

$$a_1 = -0.01(a/d)^2 + 0.07 \quad (a/d) - 0.34 \quad R=1.00 \quad \dots\dots (40)$$

By substitution in equation (38)

$$\% S = 0.16(a/d) + 0.44 + [-0.01(a/d)^2 + 0.07(a/d) - 0.34] A_s \quad \dots\dots (41)$$

Following the same procedures:

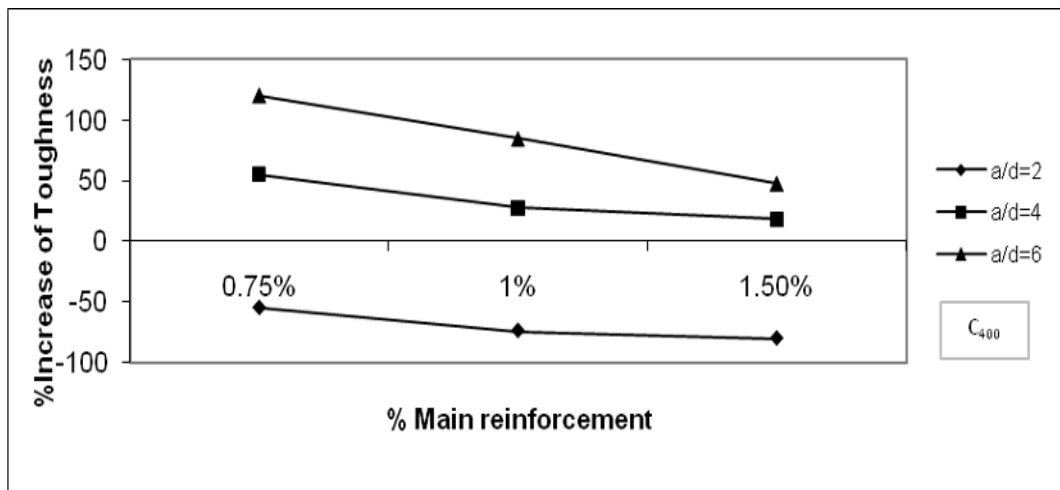


Figure 25: relation between % increase of toughness and % main reinforcement.

The relation of figure 25 can be represented by the following equations:

$$T4 = -0.13A_s - 0.44 \quad R=0.96 \quad a/d=2 \quad \dots (42)$$

$$T5 = -0.18A_s + 0.70 \quad R=0.96 \quad a/d=4 \quad \dots (43)$$

$$T6 = -0.36A_s + 1.56 \quad R=0.99 \quad a/d=6 \quad \dots (44)$$

Equations 42, 43 and 44 are represented by:

$$\% T = a_0 + a_1 A_s \quad \dots (45)$$

$a_0, a_1$  depend on  $a/d$  ratio as:

$$a_0 = 0.50 (a/d) + 1.4 \quad R=0.99 \quad \dots (46)$$

$$a_1 = -0.06(a/d) + 0.01 \quad R=0.95 \quad \dots (47)$$

By substitution in equation (45)

$$\% T = 0.5(a/d) + 1.4 + [-0.06(a/d) + 0.01] A_s \quad \dots (48)$$

**For grade 600 of concrete:**

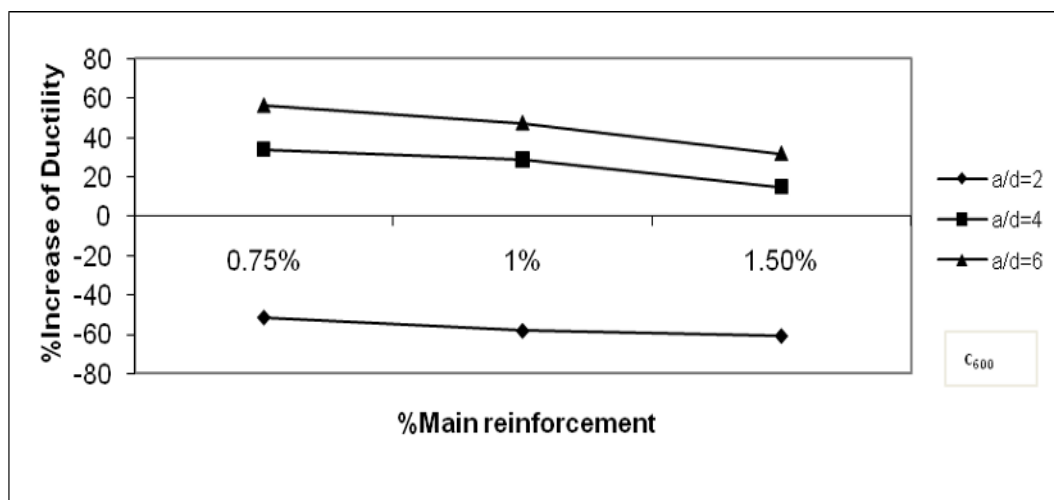


Figure 26: relation between % increase of ductility and % main reinforcement

The relation of figure 26 can be represented by the following equations:

$$D7 = -0.05A_s - 0.48 \quad R=0.97 \quad a/d=2 \quad \dots (49)$$

$$D8 = -0.10A_s + 0.44 \quad R=0.97 \quad a/d=4 \quad \dots (50)$$

$$D9 = -0.12A_s + 0.70 \quad R=0.98 \quad a/d=6 \quad \dots (51)$$

Equations 49, 50 and 51 are represented by:

$$\% D = a_0 + a_1 A_s \quad \dots (52)$$

$a_0, a_1$  depend on  $a/d$  ratio as:

$$a_0 = 0.3 (a/d) - 0.96 \quad R=0.95 \quad \dots (53)$$

$$a_1 = -0.02(a/d) - 0.02 \quad R=0.97 \quad \dots (54)$$

by substitution in equation (52)

$$\% D = 0.3(a/d) - 0.96 + [-0.02(a/d) - 0.02] A_s \quad \dots (55)$$

Following the same procedure:

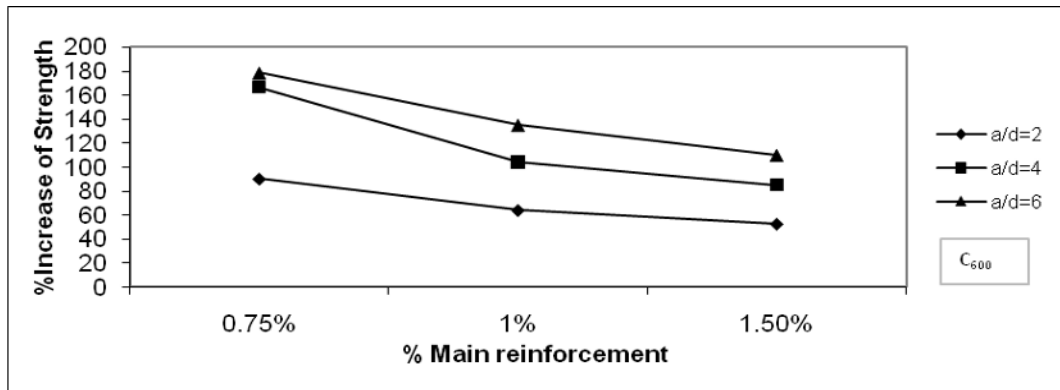


Figure 27: relation between % increase of strength and % main reinforcement

The relation of figure 27 can be represented by the following equations:

$$S7 = -0.19A_s + 1.07 \quad R=0.97 \quad a/d=2 \quad \dots\dots (56)$$

$$S8 = -0.41A_s + 2.00 \quad R=0.95 \quad a/d=4 \quad \dots\dots (57)$$

$$S9 = -0.34A_s + 2.09 \quad R=0.98 \quad a/d=6 \quad \dots\dots (58)$$

Equations 56, 57 and 58 are represented by:

$$\% S = a_0 + a_1 A_s \quad \dots\dots (59)$$

$a_0, a_1$  depend on  $a/d$  ratio as:

$$a_0 = 0.26 (a/d) + 0.70 \quad R=0.90 \quad \dots\dots (60)$$

$$a_1 = 0.04 (a/d)^2 - 0.33 (a/d) + 0.32 \quad R=1.00 \quad \dots\dots (61)$$

by substitution in equation (59)

$$\% S = 0.26(a/d) + 0.7 + [0.04(a/d)^2 - 0.33(a/d) + 0.32] A_s \quad \dots\dots (62)$$

Following the same procedures:

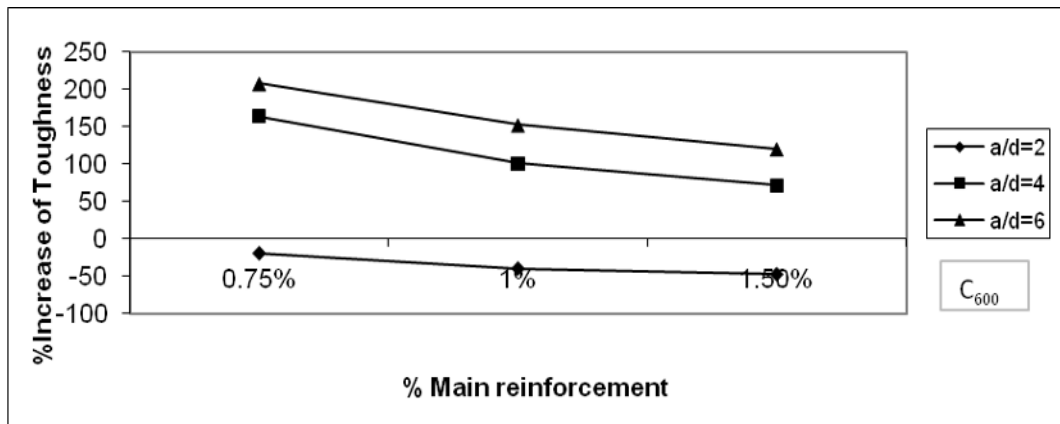


Figure 28: relation between % increase of toughness and % main reinforcement

The relation of figure 28 can be represented by the following equation:

$$T2 = -0.14A_s - 0.08 \quad R=0.97 \quad a/d=2 \quad \dots\dots (63)$$

$$T4 = -0.46A_s + 2.07 \quad R=0.97 \quad a/d=4 \quad \dots\dots (64)$$

$$T6 = -0.44A_s + 2.47 \quad R=0.98 \quad a/d=6 \quad \dots\dots (65)$$

Equations 63, 64 and 65 are represented by:

$$\% T = a_0 + a_1 A_s \quad \dots\dots (66)$$

$a_0, a_1$  depend on  $a/d$  ratio as:

$$a_0 = 0.64 (a/d) - 1.06 \quad R = 0.93 \quad \dots\dots (67)$$

$$a_1 = 0.04 (a/d)^2 - 0.42 (a/d) + 0.52 R = 1.00 \quad \dots\dots (68)$$

by substitution in equation number ..... (66)

$$\% T = 0.64(a/d) - 1.06 + [0.04(a/d)^2 - 0.42(a/d) + 0.52] A_s \quad \dots\dots (69)$$

## CONCLUSIONS

The results of the numerical analysis in this study indicated that significant increase in the flexural strength can be achieved by bonding CFRP sheets to the tension face of high strength reinforced concrete beams. As the amount of tensile steel reinforcement increases, the additional strength provided by the carbon FRP external reinforcement decreases. From the obtained results, equations are concluded to calculate the changes in ductility, strength and toughness due to the changes in  $\%A_s$ ,  $(a/d)$  ratio and grade of concrete. The gains in different characteristics are as follows:-

## DUCTILITY

In case of grade 200 ( $C_{200}$ ):

Strengthening the beams with CFRP is leading to increase the ductility of the beams by 29.4 %, 66 % and 70 % for  $\% A_s = 0.75$ ,  $\% A_s = 1.00$  and  $\% A_s = 1.50$  respectively. When  $a/d = 2$ , increase by 56.3%, 78.3% and 91.6% for  $\% A_s = 0.75$ ,  $\% A_s = 1.00$  and  $\% A_s = 1.50$  respectively when  $a/d = 4$  and increase by 77.6%, 87 and 93.3 for  $\% A_s = 0.75$ ,  $\% A_s = 1.00$  and  $\% A_s = 1.50$  respectively when  $a/d = 6$ . These results can be represented by the following formula:

$$\% D = 0.14(a/d) - 0.13 + [0.27 - 0.03(a/d)] A_s$$

In case of grade 400 ( $C_{400}$ ):

Strengthening the beams with CFRP is leading to decrease the ductility of the beams by 65%, 74.1% and 78.2 for  $\% A_s = 0.75$ ,  $\% A_s = 1.00$  and  $\% A_s = 1.50$  respectively when  $a/d = 2$ , decrease by 1.3%, 9.4% and 12.4% for  $\% A_s = 0.75$ ,  $\% A_s = 1.00$  and  $\% A_s = 1.50$  respectively when  $a/d = 4$  and increase by 28%, 18%, and 12.6% for  $\% A_s = 0.75$ ,  $\% A_s = 1.00$  and  $\% A_s = 1.50$  respectively when  $a/d = 6$ . These results can be represented by the following formula:

$$\% D = 0.24(a/d) - 1.01 + [-0.004(a/d)^2 + 0.03(a/d) - 0.11] A_s$$

In case of grade 600 ( $C_{600}$ ):

Strengthening the beams with CFRP is leading to decrease the ductility of the beams by 51.4%, 58% and 60.5 for  $\% A_s = 0.75$ ,  $\% A_s = 1.00$  and  $\% A_s = 1.50$  respectively when  $a/d = 2$ , increase 33.8%, 28.7% and 15% for  $\% A_s = 0.75$ ,  $\% A_s = 1.00$  and  $\% A_s = 1.50$  respectively when  $a/d = 4$  and increase by 56.6%, 47.6%, and 32% for  $\% A_s = 0.75$ ,  $\% A_s = 1.00$  and  $\% A_s = 1.50$  respectively when  $a/d = 6$ . These results can be represented by the following formula:

$$\% D = 0.3(a/d) - 0.96 + [-0.02(a/d) - 0.02] A_s$$

Where  $\%D$  is the percentage change of the ductility.

## Strength

In case of grade 200 ( $C_{200}$ ):

Strengthening the beams with CFRP is leading to increase the strength of the beams by 114.76 %, 76.4% and 51.2 % for %  $A_s = 0.75$ , %,  $A_s = 1.00$  and %  $A_s = 1.50$  respectively When  $a/d = 2$ , increase by 70.8%, 59.2% and 41% for %  $A_s = 0.75$ , %  $A_s = 1.00$  and %  $A_s = 1.50$  respectively when  $a/d = 4$ , increase by 56.5%, 42.7 and 27.7 for %  $A_s = 0.75$ , %  $A_s = 1.00$  and %  $A_s = 1.50$  respectively when  $a/d = 6$ . These results can be represented by the following formula:

$$\%S = 1.74 - 0.18(a/d) + [-0.02(a/d)^2 + 0.21(a/d) - 0.65] A_s$$

In case of grade 400 ( $C_{400}$ ):

Strengthening the beams with CFRP is leading to increase the strength of the beams by 51.5 %, 18.4% and 5 % for %  $A_s = 0.75$ , %,  $A_s = 1.00$  and %  $A_s = 1.50$  respectively When  $a/d = 2$ , increase by 98.5%, 71.1% and 59.6% for %  $A_s = 0.75$ , %  $A_s = 1.00$  and %  $A_s = 1.50$  respectively when  $a/d = 4$ , increase by 113%, 87% and 70% for %  $A_s = 0.75$ , %  $A_s = 1.00$  and %  $A_s = 1.50$  respectively when  $a/d = 6$ . These results can be represented by the following formula:

$$\%S = 0.16(a/d) + 0.44 + [-0.01(a/d)^2 + 0.07(a/d) - 0.34] A_s$$

In case of grade 600 ( $C_{600}$ ):

Strengthening the beams with CFRP is leading to increase the strength of the beams by 90.16 %, 63.7% and 52.5% for %  $A_s = 0.75$ , %  $A_s = 1.00$  and %  $A_s = 1.50$  respectively When  $a/d = 2$ , increase by 166.4%, 103.9% and 85% for %  $A_s = 0.75$ , %  $A_s = 1.00$  and %  $A_s = 1.50$  respectively when  $a/d = 4$ , increase by 178.3%, 135% and 110% for %  $A_s = 0.75$ , %  $A_s = 1.00$  and %  $A_s = 1.50$  respectively when  $a/d = 6$ . These results can be represented by the following formula:

$$\%S = 0.26(a/d) + 0.7 + [0.04(a/d)^2 - 0.33(a/d) + 0.32] A_s$$

Where %S is the percentage change of the Strength.

## Toughness

In case of grade 200 ( $C_{200}$ ):

Strengthening the beams with CFRP is leading to increase the toughness of the beams by 127%, 165.8% and 123.8% for %  $A_s = 0.75$ , %  $A_s = 1.00$  and %  $A_s = 1.50$  respectively When  $a/d = 2$ , increase by 160%, 195.6% and 168.9% for %  $A_s = 0.75$ , %  $A_s = 1.00$  and %  $A_s = 1.50$  respectively when  $a/d = 4$ , increase by 190.4%, 162.2% and 132.8% for %  $A_s = 0.75$ , %  $A_s = 1.00$  and %  $A_s = 1.50$  respectively when  $a/d = 6$ . These results can be represented by the following formula:

$$\%T = 0.51(a/d) - 1.03 + [-0.44(a/d) + 2.57] A_s + [0.09(a/d) - 0.6] A_s^2$$

In case of grade 400 ( $C_{400}$ ):

Strengthening the beams with CFRP is leading to decrease the toughness of the beams by 54.8%, 73.8% and 80.1% for %  $A_s = 0.75$ , %  $A_s = 1.00$  and %  $A_s = 1.50$  respectively When  $a/d = 2$ , increase by 54.6%, 27% and 18.1% for %  $A_s = 0.75$ , %  $A_s = 1.00$  and

$\%A_s=1.50$  respectively when  $a/d = 4$ , increase by 120%, 84.4% and 47.6% for  $\% A_s = 0.75$ ,  $\% A_s=1.00$  and  $\%A_s=1.50$  respectively when  $a/d = 6$ . These results can be represented by the following formula:

$$\%T = 0.5(a/d) + 1.4 + [-0.06(a/d) + 0.01] A_s$$

In case of grade 600 ( $C_{600}$ ):

Strengthening the beams with CFRP is leading to decrease the toughness of the beams by 19.9%, 40% and 47.5% for  $\%A_s = 0.75$ ,  $\%A_s=1.00$  and  $\%A_s=1.50$  respectively. When  $a/d = 2$ , increase by 162.7%, 99.9% and 71.2% for  $\% A_s = 0.75$ ,  $\% A_s=1.00$  and  $\%A_s=1.50$  respectively when  $a/d = 4$ , increase by 207.3%, 151.6% and 119.4% for  $\% A_s = 0.75$ ,  $\% A_s=1.00$  and  $\%A_s=1.50$  respectively when  $a/d = 6$ . These results can be represented by the following formula:

$$\%T = 0.64(a/d) - 1.06 + [0.04(a/d)^2 - 0.42(a/d) + 0.52] A_s$$

Where  $\%T$  is the percentage change of the toughness.

## REFERENCES

1. Khairy Hassan Abdelkareem "Analytical Study on Seismic Resistant Characteristics of RC Bridge piers" Thesis for doctor of Engineering Degree, Saitama University, Tokyo, Japan, March 1999
2. Khairy Hassan Abdelkareem "Analytical Study on Seismic Resistant Characteristics of RC Bridge piers" Thesis for doctor of Engineering Degree, Saitama University, Tokyo, Japan, March 1999
3. Khairy Hassan, "Some Main Factors Affecting Efficiency of Externally Bonded Partially Lateral Wrapping CFRP Short Static Loading Plain and R.C. Column" Journal of Engineering Sciences, Assiut University, Vol. 35, No. 5, September 2007
4. Khairy Hassan Abdelkareem "Experimental Study on Seismic Performance of RC Bridge Columns Strengthened by FRP Aramid sheets. Part 1" Bulletin of the Faculty of Engineering, Assiut University, Vol. 28, No. 2, May 2000, pp. 1-14
5. Omar F. and Khairy Hassan A., "Repair of R.C. Cracked Beams Using Externally Bonded CFRP Sheets" 10th International Colloquium on Structural and Geotechnical Engineering, April 22-24, 2003, Ain Shams University, Cairo, Egypt.
6. N. F. Grace, G. A. Sayed, A. K. Soliman and K. R. Saleh, (1999) "Strengthening Reinforced Concrete Beams Using Fiber Reinforced Polymer (FRP) Laminates", ACI Structural Journal ACI Structural Journal, V. 96, No. 5.
7. Amer M. Ibrahim and Amer M. Ibrahim (2009) "Finite Element Modeling of Reinforced Concrete Beams Strengthened with FRP Laminates", European Journal of Scientific Research ISSN 1450-216X Vol.30 No.4, pp.526-541.
8. J. Lundqvist, H. Nordin, B. Täljsten, and T. Olofsson (2005) "NUMERICAL ANALYSIS OF CONCRETE BEAMS STRENGTHENED WITH CFRP— A STUDY OF ANCHORAGE LENGTHS" Proceedings of the International Symposium on Bond Behaviour of FRP in Structures.

9. YasmeeenTalebObaidata, Susanne Heydena, Ola Dahlbloma, Ghazi Abu-Farsakhb and Yahia Abdel-Jawadb(2010)"Retrofitting of Reinforced Concrete Beams using Composite Laminates" Structural Mechanics, LTH, Sweden.
10. Mohammed Jassam Mohammed Altaee(2011)" Effect of CFRP Plate Location on Flexural Behavior of RC Beam Strengthened with CFRP Plate" Proceeding of the International Conference on Advanced Science, Engineering and Information Technology .
11. Reza Mahjoub and Seyed Hamid Hashemi(2010)" Finite Element Analysis of RC Beams Strengthened with FRP Sheets under Bending" Australian Journal of Basic and Applied Sciences, 4(5): 773-778.
12. ANSYS , ANSYS User's Manual .
13. Kachlakev, D.I. and McCurry, D., Jr.,(2000) Simulated Full Scale Testing of Reinforced Concrete Beams Strengthened with FRP Composites: Experimental Results and Design Model Verification, Oregon Department of Transportation, Salem, Oregon,
14. Kaw, A. K., (1997) Mechanics of Composite Materials, CRC Press LLC, Boca Raton, Florida.
15. Kachlakev Damian, Miller Thomas, and Yim Solomon, (2001)'Finite Element Modeling of Reinforced Concrete Structures Strengthened with FRP Laminates' Report for regon Department Of Transportation, Salem,.
16. American Society for Testing and Materials (ASTM)(1983) Subcommittee C09.64, Standard Test Method for Pulse Velocity Through Concrete, Designation C 597-83, ASTM, West Conshohocken, Pennsylvania.
17. American Society for Testing and Materials (ASTM)(1994) Subcommittee C09.70, Standard Test Method for Static Modulus of Elasticity and Poisson's Ratio of Concrete in Compression, Designation C 469-94, ASTM, West Conshohocken, Pennsylvania.

## دراسة نظرية في سلوك الإنحناء للكمرات الخرسانية المسلحة المقواه خارجياً

### برقائق الواح الكربون

في كثير من الاحيان تحتاج الهياكل الخرسانية للمنشآت لاصلاحات او ترميمات نتيجة لزيادة الاحمال الحية لهذا المنشأ او لوجود صدأ في حديد التسليح او لوجود اخطاء في التنفيذ او لحدوث بعض الحوادث مثل الزلازل. وهناك طرق كثيره تستخدم في ترميم المنشآت الخرسانية منها التدعيم باستخدام الواح من الصلب والتدعيم باستخدام شرائح من الياف الكربون المسلح . وتعتبر الطريقه الاخيره من افضل الطرق حيث انها تتميز بالقوة المرتفعة ومقاومتها للصدأ وكذلك خفة وزنها.

و من هنا يقدم هذا البحث دراسة نظرية لتقييم السلوك الانشائي للكمرات الخرسانية المسلحة والمقواه باستخدام رقائق من الياف الكربون تحت تاثير حمل الانحناء .

و المتغيرات الرئيسية التي تمت دراستها هي رتبة الخرسانة وطول الكمرتين ونسبة حديد التسليح الرئيسي. تم من خلال هذا البحث عمل نماذج للكمرات الخرسانية المسلحة والمقواه باستخدام شرائح من ألياف الكربون



لدراسة سلوك الإحناء على تلك الكمرات الخرسانية عند تغير بعض خواص هذه الكمرات وذلك باستخدام برنامج التحليل العددي (Ansys).

تم دراسة تأثير تغير تلك الخواص على سلوك الكمرات ممثلاً في :

1-المطولية (Ductility)

2-المقاومة (Strength)

3-المتانة (Toughness)

وقد تم استنتاج معادلات رياضية تعطي التغير في تلك الخواص نتيجة للتقوية باستخدام رقائق من الياف الكربون مقارنة بالكمرات المناظرة بدون تقوية .